Journal of Science and Technology in Civil Engineering, HUCE, 2023, 17 (2): 120–132

BUILDING DROUGHT CLASSIFICATION MAP WITH LANDSAT 8 IMAGE DATA IN BAC BINH DISTRICT, BINH THUAN PROVINCE

Luu Thi Dieu Chinh[a], Ha Thi Hang[b,*], Bui Duy Quynh[b], Dao Duy Toan[b]

[a]*Faculty of Hydraulic Engineering, Hanoi National University of Civil Engineering, 55 Giai Phong road, Hai Ba Trung district, Hanoi, Vietnam*
[b]*Faculty of Bridges and Roads, Hanoi National University of Civil Engineering, 55 Giai Phong road, Hai Ba Trung district, Hanoi, Vietnam*

Article history:
Received 14/5/2023, Revised 07/6/2023, Accepted 14/6/2023

Abstract

Vietnam experiences increasing droughts throughout the dry season due to climate change, global warming, and human-caused activities like urbanization and deforestation. Drought hazard significantly impacts socioeconomic, agriculture, and the environment; it directly threatens human lives, livelihoods, food security, and environmental degradation. It is essential to have a drought assessment map to assist in developing and implementing strategies to combat drought. Space remote sensing technology development has enabled efficient and cost-effective monitoring and evaluation of droughts on a large scale, surpassing the capabilities of ground-based observations. This research uses remote sensing technology to monitor and assess the severity of the drought in the Bac Binh district, Binh Thuan province. We analyzed the Temperature Vegetation Dryness Index (TVDI) using multi-temporal Landsat 8 satellite data for the severe drought events in 2014, 2017, and 2020. The results indicate a significant increase in the percentage of land area affected by drought, from 50.74% in 2014 to 66.23% in 2020. The obtained maps provide valuable visual data to relevant agencies, assisting with planning preventative measures and mitigating future drought risks.

Keywords: drought; Landsat 8; temperature vegetation dryness index; Bac Binh.

https://doi.org/10.31814/stce.huce2023-17(2)-11

1. Introduction

Drought is a natural hazard that occurs when there is an intense and persistent shortage of precipitation [1]. Drought is especially a common phenomenon in Asia which is a living continent of more than half of the world's population [2, 3]. Since the late 1990s and continuing to the present, most of Asia, Southern Europe, Africa, and Southern Australia have shown a trend toward increasingly frequent drought occurrences [4]. In terms of the number of people affected by drought, Asia has more than 1.3 billion people affected during the same period [5]. In recent years, droughts in Asia have become more severe and frequent because of climate change and increasing water demand [6]. Droughts can have significant impacts on ecosystems and human populations, leading to crop failures, food shortages, water scarcity, and even migration and conflict [7]. The traditional method of monitoring drought is to observe and record physical indicators such as rainfall, water levels in rivers, and soil moisture from the meteorological stations [8]. This approach often relies on ground-based stations which can be time-consuming and labor-intensive, and not effective for the large scale [9]. Despite these limitations, traditional drought monitoring methods are still important in many regions where advanced technology is not widely available or accessible [10]. Meanwhile, the use of remote sensing data in monitoring drought can provide valuable information to help authorities plan and

*Corresponding author. *E-mail address:* hanght@huce.edu.vn (Hang, H. T.)

implement effective measures to mitigate the impacts of drought on the local community [11]. Nowadays, Landsat 8 satellite image data can completely overcome the limitations of traditional methods in monitoring and evaluating drought [12]. It can provide a synoptic and comprehensive view of the area, allowing for the detection of changes in vegetation health, land surface temperature, and precipitation patterns [13]. Additionally, Landsat 8 satellite image data can be collected regularly which enables the monitoring of drought over time and the assessment of its impacts on vegetation and the environment [14]. Moreover, this satellite image data is non-destructive and can cover large areas, making it cost-effective and efficient in comparison to ground-based observations [15]. With the advancement of Landsat satellite generations, the accuracy and spatial resolution of this new-generation data have strongly improved, allowing for more precise and reliable drought monitoring [16]. These advantages have made Landsat 8 satellite image data an essential tool for monitoring drought and informing decision-making in various sectors such as agriculture, water management, and disaster risk reduction [17]. Bac Binh district is located in the Northeastern of Binh Thuan province, Vietnam. It has a strategic position because of its location at the intersection of the Central Highlands and the coastal region of Southern Vietnam [18]. Moreover, it has a diverse landscape and a rich cultural heritage and is home to many ethnic minority groups [19]. Nevertheless, it is situated in a dry and arid region, making it particularly vulnerable to drought [20]. Although the severity of the drought varied over different years, it has caused damage to people's life, people livelihood, and local economic development [21]. Determination of drought using the satellite image data can rely on various indices such as the Normalized Difference Vegetation Index (NDVI), the Soil Adjusted Vegetation Index (SAVI), the Temperature Vegetation Dryness Index (TVDI), and the Vegetation Condition Index (VCI) [22]. These indices are often utilized to detect changes in vegetation cover, soil moisture, and surface temperature [23]. Meanwhile, TVDI is a significant index for drought monitoring because it can combine information on land surface temperature and vegetation health to provide a measure of the moisture stress of the landscape [24]. In addition, TVDI can capture the onset of drought earlier than other indices because it detects the effects of water stress on vegetation before they occur [25]. TVDI is also sensitive to changes in temperature, which is an important factor in drought formation [24, 26]. Thus, TVDI is considered an effective index for detecting droughts in different regions, and its results can be easily interpreted and mapped [27]. As a result, this index has often been used in monitoring drought [21, 26, 28–32]. Nonetheless, most of these studies used old-generation Landsat satellite images to monitor drought [21, 26, 31], or used different satellite image data in assessing drought [28–30, 32]. Whereas the old-generation Landsat imagery data was often delayed for a long time before being provided to users, which hindered timely and efficient analysis [33]. Different satellite image data can lead to variations in the TVDI values, which can affect the accuracy and reliability of the drought assessment [34].Therefore, this study applied multi-temporal Landsat 8 satellite data to monitor and evaluate drought conditions in Bac Binh district, Binh Thuan province, in 2014, 2017, and 2020 based on the Temperature Vegetation Dryness Index (TVDI). The calculated TVDI index from the same satellite image data can limit potential inconsistencies when using different satellite image data. The received maps of this study can provide valuable information for monitoring drought and help relevant authorities plan and implement effective measures to minimize the impact of drought on the local community.

2. Material and Methods

2.1. Study area

Bac Binh district is the largest district in Binh Thuan province, located in the north of Binh Thuan province, about 230 km East of Ho Chi Minh City and about 200 km Southwest of Nha Trang

(Fig. 1). Bac Binh district has a natural area of about 1872.2 km2 and is located from 10°58’27"to 11°31’38"North latitude, 108°06’30"to 108°37’34"East longitude.

The terrain of Bac Binh district is quite complex, with a small flat area sandwiched between mountain ranges in the North and Northwest and dunes in the Southeast, forming a basin-like terrain [35]. The district is located in the tropical monsoon climate zone, with plenty of sunshine, wind, no winter, and the driest climate in Vietnam. The climate is divided into two distinct seasons: the rainy season and the dry season. The rainy season usually starts from May to October, while the dry season is from November to April of the following year. In reality, the rainy season only focuses on three months: August, September, and October, so the dry season lasts longer [36]. Desertification of sand dunes has been the primary form of land degradation in the Bac Binh district in recent years [20].

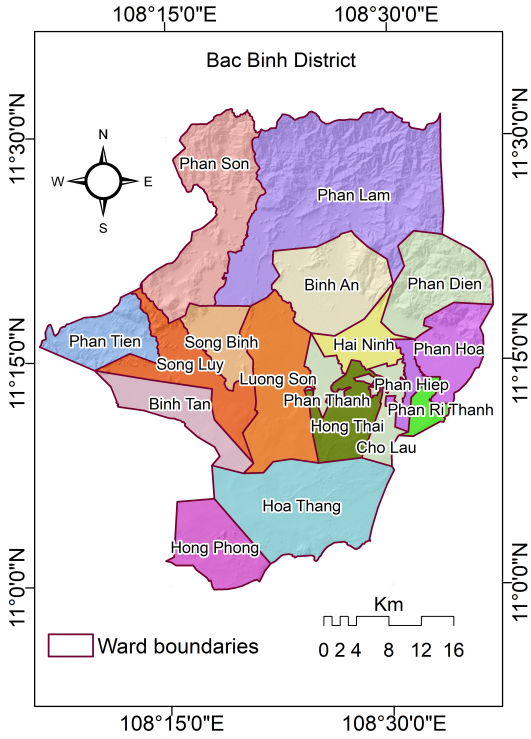

Figure 1. The study area

2.2. *Data used*

The Landsat 8 optical satellite imagery is a source of satellite data with moderate spatial resolution, completely free, and regularly updated (Table 1). Its abundant spectral channels allow for application in many studies on natural resources, the environment, hydrology, and meteorology at the district scale and above [16].

Table 1. Detailed information of Landsat 8 images [37]

Bands	Wavelength (micrometers)	Spatial resolution (meters)	Temporal resolution (days)	Sensor type
Band 1 - Coastal aerosol	0.43–0.45	30	16	OLI
Band 2 - Blue	0.45–0.51	30	16	OLI
Band 3 - Green	0.53–0.59	30	16	OLI
Band 4 - Red	0.64–0.67	30	16	OLI
Band 5 - Near Infrared (NIR)	0.85–0.88	30	16	OLI
Band 6 - Shortwave Infrared (SWIR) 1	1.57–1.65	30	16	OLI
Band 7 - Shortwave Infrared (SWIR) 2	2.11–2.29	30	16	OLI
Band 8 - Panchromatic	0.50–0.68	15	16	OLI
Band 9 - Cirrus	1.36–1.38	30	16	OLI
Band 10 - Thermal Infrared (TIRS) 1	10.6–11.19	100	16	TIRS
Band 11 - Thermal Infrared (TIRS) 2	11.50–12.51	100	16	TIRS

In this study, the Landsat 8 data was downloaded from the website of the United States Geological Survey [38]. The satellite images were acquired during the driest period in the Bac Binh district from

January to March (Table 2).

Table 2. The used Landsat 8 data

No	Data type	Scene name	Data acquisition time
1	Landsat 8 OLI	LC08_L1TP_124052_20140130_20200912_02_T1	January 30, 2014
2	Landsat 8 OLI	LC08_L1TP_124052_20170207_20200905_02_T1	February 07, 2017
3	Landsat 8 OLI	LC08_L1TP_124052_20200216_20200823_02_T1	February 16, 2020

2.3. Methodology

The research methodology consists of four main steps and is described in Fig. 2.

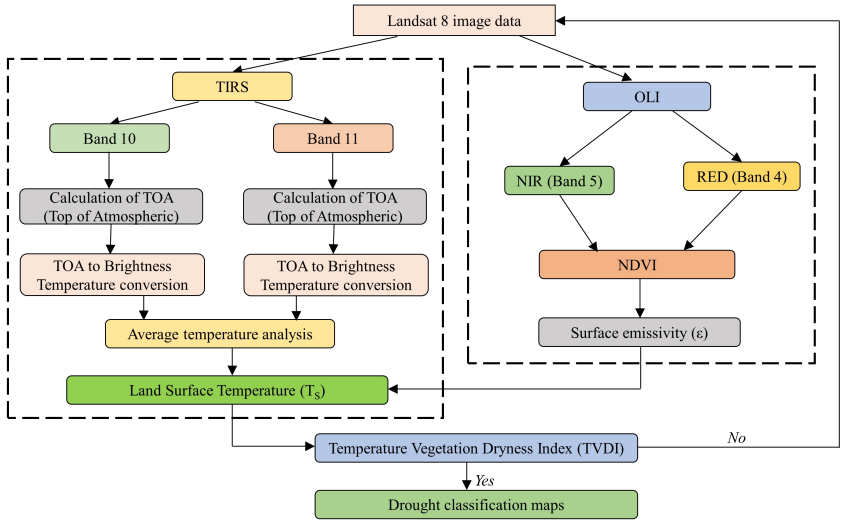

Figure 2. The methodology used in this study

a. Step 1. Calculation of Normal Difference Vegetation Index (NVDI)

The NDVI is an important parameter in agriculture, used to indirectly monitor rainfall, evaluate the impact of weather, and calculate biomass, seasonal productivity, and plant health [39]. The NDVI indicates the degree of vegetation cover on the Earth's surface and often ranges from −1 to 1 [40]. The higher the NDVI is, the higher the vegetation density is, and in reverse [41]. In this study, the NDVI was calculated as the following equation:

$$NDVI = \frac{NIR - Red}{NIR + Red} \tag{1}$$

where *NIR, Red* refer to the near-infrared and red wavelengths of the electromagnetic spectrum, respectively. These values correspond to band 5 and band 4 of Landsat 8 data (Table 1).

b. Step 2. Calculation of Land Surface Temperature (LST)

To calculate land surface temperature, the following steps need to be taken [42]:

- Converting digital number values (DNs) on Landsat images in the thermal infrared channel to top-of-atmosphere reflectance (TOA) values using the following formula:

$$TOA = M_L.Q_{cal} + A_L \tag{2}$$

where M_L is band-specific multiplicative rescaling factor from the metadata; Q_{cal} corresponds to band 10 and band 11; A_L repsresents band-specific additive rescaling factor from the metadata.

- TOA to Brightness Temperature conversion (T_B):

$$T_B = \frac{K_2}{ln\left(1 + \frac{K_1}{L_\lambda}\right)} - 273.15 \tag{3}$$

where K_1 is band-specific thermal conversion constant from the metadata; K_2 is band-specific thermal conversion constant from the metadata; L_λ is TOA value.

Table 3. Information on radiation values of Landsat-8 satellites

Value	Band 10	Band 11
ML	0.0003342	0.0003342
AL	0.1	0.1
K1	774.8853	480.8883
K2	1321.0789	1201.1442

- Calculation of the surface emissivity (ε):

The surface emissivity can be determined from remote sensing data based on the reclassifying results of land cover types or the NDVI factor. Surface emissivity indicates the ability of a surface to emit thermal radiation [43]. The thermal bands of Landsat 8 data capture the emitted radiation from the Earth's surface, and accurate estimation of surface emissivity is crucial for retrieving surface temperature and analyzing the thermal properties of different land cover types [44]. The determination of the surface emissivity based on the NDVI can identify the surface emissivity in detail for each pixel and heterogeneous area. In this study, the surface emissivity of a pixel is calculated as follows [42]:

$$\varepsilon = \varepsilon_v P_v + \varepsilon_s (1 - P_v) \tag{4}$$

where ε_v and ε_s are characteristic emissivities for pure vegetation cover area (= 0.985) and homogeneous soil (= 0.960), respectively [45]; P_v is the proportion of vegetation cover in a pixel, and ranges from 0 for bare soil to 1 for vegetation. The value of P_v is determined using the formula [46]:

$$P_v = \left[\frac{NDVI - NDVI_{\min}}{NDVI_{\max} - NDVI_{\min}}\right]^2 \tag{5}$$

- The Land Surface Temperature (TS) was calculated using the below equation:

$$T_S = \frac{T_B}{1 + \left(\frac{\lambda . T_B}{\rho}\right) ln(\varepsilon)} \tag{6}$$

where λ is the central wavelength of the thermal infrared channel; $\rho = h\frac{c}{\sigma}$; σ is Stefan-Boltzmann constant (= 1.38×10^{-23} $\frac{J}{K}$); h is Plank constant (= 6.626×10^{-34} J.sec); c is light speed (= 299792458 m/s);

c. Step 3. Calculation of Temperature Vegetation Dryness Index (TVDI)

TVDI is a remote sensing index that was developed to assess vegetation health and soil moisture levels based on temperature and vegetation data [26]. Sandholt et al. suggested the calculation of TVDI by combining the land surface temperature and NDVI (Normalized Difference Vegetation Index) [47]. By measuring the difference between the land surface temperature and the temperature of the vegetation, TVDI can provide an estimate of the degree of dryness or wetness in the soil [48]. According to that, TVDI can be calculated by using the following equation [47]:

$$TVDI = \frac{T_S - T_{S\,\min}}{T_{S\,\max} - T_{S\,\min}} \tag{7}$$

where T_S is the calculated surface temperature (in degrees Celsius); $T_{S\,\max}$ and $T_{S\,\min}$ are maximum and minimum surface temperatures. respectively (in degrees Celsius);

d. Step 4. Creation of drought maps

The drought maps were classified based on the calculated TVDI index. Typically. the TVDI ranges from 0 to 1 and indicates the status of drought at different levels [49]. The drought level is classified in Table 4.

Table 4. Classification of drought levels based on the TVDI [47]

No	TVDI value	Drought level
1	0.0 – 0.2	No drought
2	0.2 – 0.4	Low drought
3	0.4 – 0.6	Moderate drought
4	0.6 – 0.8	Severe drought
5	0.8 – 1.0	Very severe drought

3. Results and discussion

3.1. Normal Difference Vegetation Index (NVDI) maps

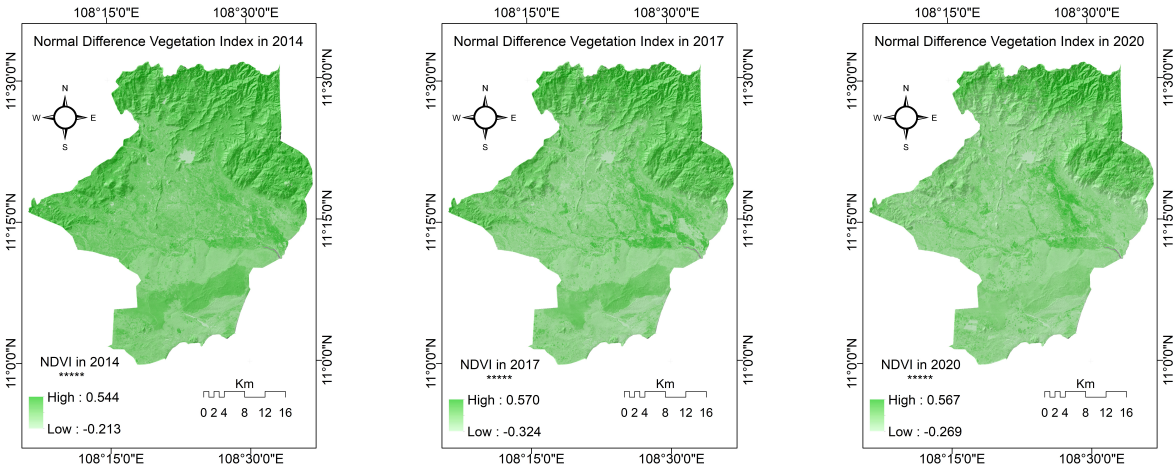

(a) 2014 (b) 2017 (c) 2020

Figure 3. NDVI maps in 2014, 2017, and 2020

In this study, NDVI maps were generated based on band 4 and band 5 of Landsat 8 satellite data in 2014, 2017, and 2020 (Fig. 3). NDVI values ranged from (−0.213) to 0.544 in 2014, from (−0.324) to 0.570 in 2017, and from (−0.269) to 0.567 in 2020, respectively. This result seems to show that the vegetation coverage within the study area has not increased much. It can be observed that over time, the average value of NDVI across the study area shows a decrease, indicating a decline in vegetation cover in the Bac Binh district. Fig. 3 highlights a significant change in NDVI, particularly in the central and southern areas, where water shortages for agricultural production and desertification are becoming more pronounced, respectively. This finding aligns completely with the observed vegetation loss in the Land-cover classes maps from a previous study conducted by Dang et al. in 2020 [35]. Furthermore, the diminishing occurrence of high NDVI values in the northern part of the Bac Binh district confirms the significant decline in the forests of the north.

3.2. Land Surface Temperature (LST) maps

Similar to NDVI, LST maps were built based on band 10 and band 11 of Landsat 8 satellite data in 2014, 2017, and 2020 (Fig. 4). LST values ranged from 16.7 to 36.3 °C in 2014, from 17.6 to 39.8 °C in 2017, and from 21.5 to 42.4 °C in 2020, respectively.

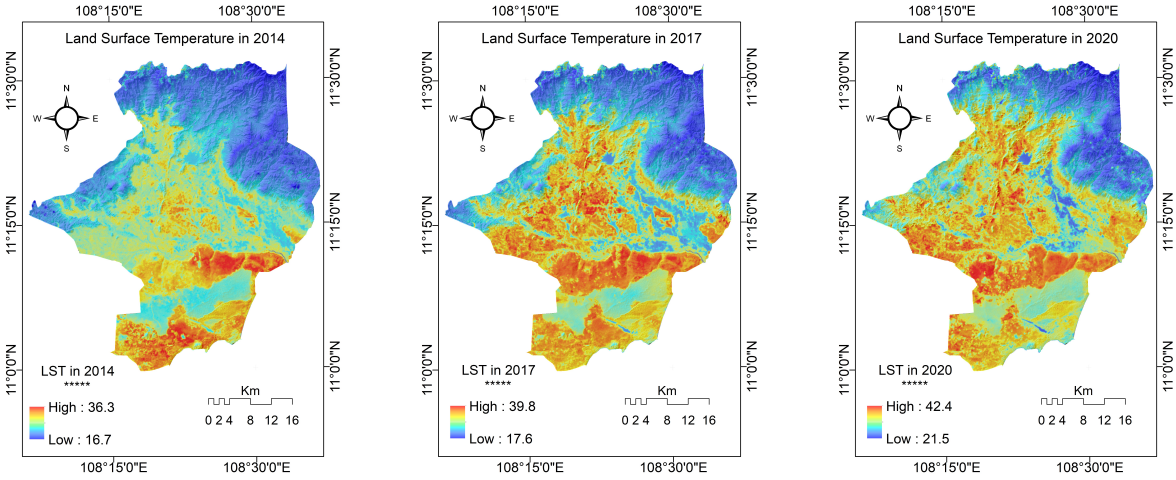

(a) 2014 (b) 2017 (c) 2020

Figure 4. LST maps in 2014, 2017, and 2020

The temperature maps depicted in Fig. 4 reveal a significant increase in surface temperature across the entire Bac Binh district, with particular emphasis on the central area. The observed temperature rise in the western and northern forests, as illustrated in Fig. 4, aligns perfectly with the documented decrease in vegetation cover between 2009-2014 and 2014-2019 reported by Dang et al. (2020) [35]. The variation in absolute temperature values between this study and the literature [35] primarily arises from the use of different image sources and analytical data. However, in terms of spatial patterns, the classification of surface temperature exhibits a similarity between the current study and the previous study, despite relying on only a single image to represent dry season data in this study.

It is noteworthy that the increase in surface temperature between 2014 and 2017 appears to be significantly higher compared to the period of 2017-2020. This discrepancy can be attributed to the active El Niño period between 2014-2017, while the period of 2017-2020 corresponds to an active phase of the La Niña weather pattern. The agreement between the studied land surface temperature maps and those of the previous literature confirmed the reliability of the research outcomes.

3.3. Temperature Vegetation Dryness Index (TVDI) maps

TVDI reflects the normalized surface temperature ratio calculated from LST using Eq. (7) to better represent the variation of land surface temperature. TVDI values ranged from 0 to 1, and the higher these values are, the greater the degree of drought is, and in reverse. The maps of TVDI of Bac Binh district in 2014, 2017, and 2020 are presented in Fig. 5. The TVDI map for the years 2014, 2017, and 2020 illustrates the correlated changes in surface temperature across the study area. It is evident that the northern purple area (TVDI ≈ 0) gradually diminishes and nearly disappears towards the west, while expanding in the central area (refer to Fig. 5(b)). This surface temperature response corresponds to the decline in vegetation cover in the northern and western regions, accompanied by an increase in cultivated areas in the central region. Furthermore, the southern region experiences an expansion of the area with high TVDI values, indicating the spreading of sand dunes. Despite the absence of validation data, the results of the TVDI map for the Bac Binh area in 2019 (Fig. 5(b)) exhibit a similar pattern when compared to the NDDI (Normalized Difference Drought Index) map reported by Trinh and Vu (2019) [20]. This similarity provides further support for the reliability of the paper's findings.

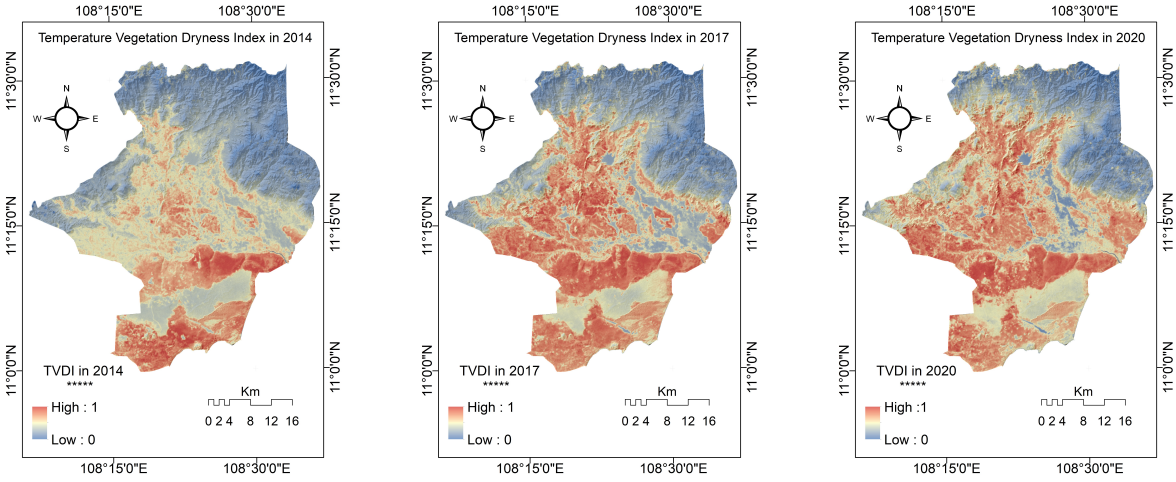

(a) 2014 (b) 2017 (c) 2020

Figure 5. TVDI maps in 2014, 2017, and 2020

3.4. Drought classification maps

Based on the analysis of the TDVI values, drought classification maps were created. Then, the drought classification maps of the Bac Binh district of Binh Thuan province in 2014, 2017, and 2020 are presented in Fig. 6.

The results show that most of the study area has a moderate to very high level of drought. Areas with no drought and low drought were mainly concentrated in the north, where natural forest coverage remains. However, the area of these regions during the period 2014-2020 tended to decrease significantly along with the decrease in the natural forest area. The area of these regions was 92216.8 ha (49.26%) in 2014, followed by 71386.8 ha (38.13%) in 2017, and followed by 63225.6 ha (33.77%), respectively. Comparing between 2014 and 2017, the area of these regions decreased by 20830.0 ha (11.13%), while comparing between 2017 and 2020, it decreased by 8161.2 ha (4.36%) (detailed in Table 5 and Fig. 7).

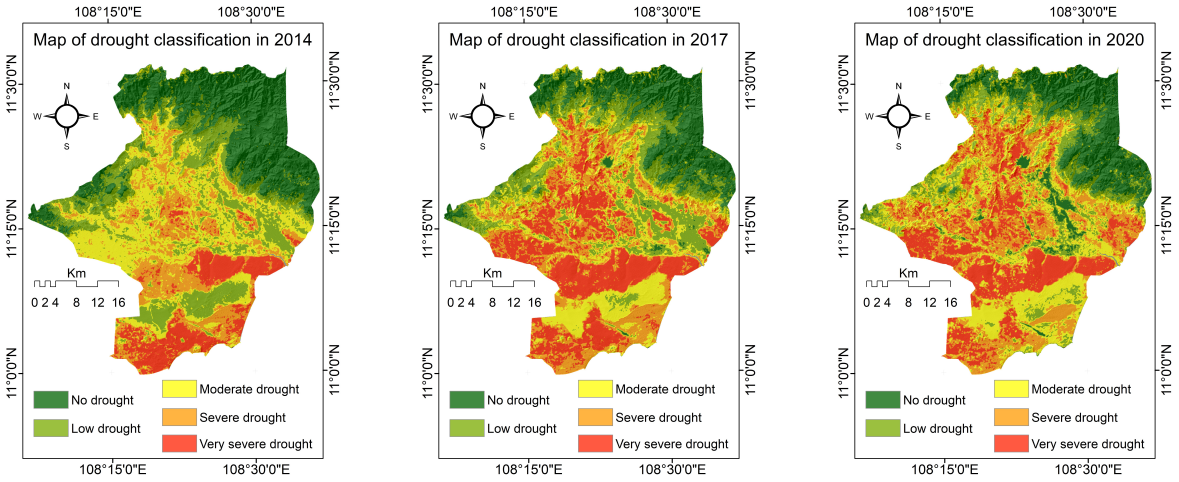

(a) 2014 (b) 2017 (c) 2020

Figure 6. Drought classification maps in 2014, 2017, and 2020

Table 5. Statistical data of drought classification areas in 2014, 2017, and 2020

Classification drought	The year 2014		The year 2017		The year 2020	
	Area (ha)	Area (%)	Area (ha)	Area (%)	Area (ha)	Area (%)
No drought	49102.5	26.23	34078.6	18.20	34197.1	18.27
Low drought	43114.3	23.03	37308.2	19.93	29028.5	15.51
Moderate drought	45339.9	24.22	35672.0	19.05	42779.5	22.85
Severe drought	30867.7	16.49	39861.8	21.29	45679.6	24.40
Very severe drought	18794.7	10.04	40298.4	21.52	35534.3	18.98

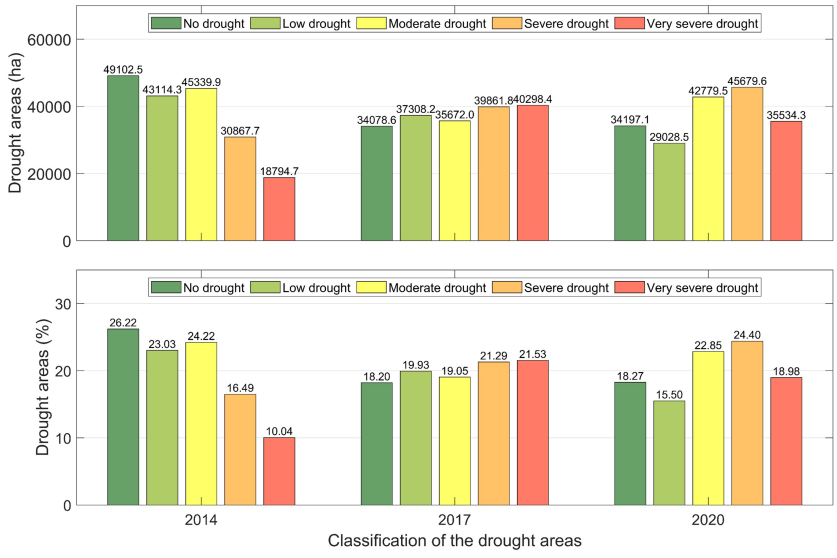

Figure 7. Areas of drought in hectares and percentages by classification

Meanwhile, the area experiencing moderate to severe drought increased significantly from 2014 to 2020 and was mainly concentrated in agricultural production areas and sandy soils. In 2014, the area of these regions accounted for 95002.3 ha (50.74%). However, these regions had expanded to 115832.3 ha (61.87%) in 2017. This expansion was mainly attributed to the impact of El Nino in 2016. Furthermore, the drought-affected area continued to grow by approximately 4.3%, accounting for 123993.5 ha (66.23%) in 2020 due to the expansion of sandy soil area and a decrease in agricultural land. Thus, it is evident that within a short period from 2014 to 2020, the area experiencing moderate drought to very severe drought increased quite rapidly. In 2014, these areas only accounted for half of the total area of the district, by 2020, they accounted for two-thirds of the total area of the district. The drought maps analyzed in this study exhibit significant differences from the drought map of the Bac Binh district published by Trinh and Vu (2019) [20]. The main disparity arises from utilizing the TVDI index in this study, while Trinh and Vu relied on the NDDI index without incorporating land surface temperature data. Additionally, the classification thresholds for these two indicators are entirely distinct. However, despite these disparities, there is a notable increase in the extent of moderate to severe drought, with a roughly 7% rise from 2011 to 2017, as reported by Trinh and Vu [20]. This finding supports the reasonable conclusion that the research results reflect the increasing trend of dry areas over time. Furthermore, it is noteworthy that the soil moisture and land surface temperature monitoring points depicted in Fig. 5 [20] are situated entirely within the regions experiencing moderate to very severe drought, as identified in this report. This observation further confirms the reasonableness and reliability of employing the TVDI for drought assessment in this study.

Generally, the drought in Bac Binh district, Binh Thuan province, is increasing both in movement speed and area expansion, and this phenomenon seriously affects the quality of life, living environment, and livelihoods of local people. In addition to the unfavorable terrain, prolonged hot weather conditions and low rainfall increase the temperature in the area, and the reduction of vegetation coverage is also the main reason leading to the drought in the research area.

4. Conclusions

In this study, multi-temporal Landsat 8 satellite data were used to assess drought conditions in Bac Binh district, Binh Thuan province, for the years 2014, 2017, and 2020 based on the Temperature Vegetation Dryness Index (TVDI). The results indicate that areas without drought and with low drought levels are primarily located in the northern part of the study area, where natural forest coverage still exists. However, these regions are experiencing a significant decrease in size. Moderate to very severe drought areas are concentrated in the central and southern parts of the study area, characterized by basin-like terrain and predominantly sandy soil, and are also the location of local people's production activities. The study results demonstrate the expansion in both the extent and severity of drought from 2014 to 2020. The percentage of drought-affected areas has notably increased from 50.74% in 2014 to 66.23% in 2020. The drought situation is predicted to worsen in 2023 with the incoming El Nino event. This study also highlights the effectiveness of remote sensing data in monitoring and assessing drought conditions over a large area and an extended period. The drought maps can serve as a valuable tool for local authorities to develop policies to mitigate drought risks, preserve natural forest areas, and guide appropriate livelihood changes for the local population. In future work, multi-remote sensing images covering a longer period, coupled with in-situ observations and land cover classification maps, can be used to further enhance the classification of drought levels in Bac Binh province with reduced uncertainty.

Acknowledgments

This study was sponsored by Hanoi University of Civil Engineering for the Research Group "Research on GIS & RS technology in disaster mitigation and adaptation to climate change".

References

[1] Zargar, A., Sadiq, R., Naser, B., Khan, F. I. (2011). A review of drought indices. *Environmental Reviews*, 19(NA):333–349.

[2] Miyan, M. A. (2015). Droughts in asian least developed countries: vulnerability and sustainability. *Weather and Climate Extremes*, 7:8–23.

[3] Ismail, Z., Go, Y. I. (2021). Fog-to-water for water scarcity in climate-change hazards hotspots: pilot study in Southeast Asia. *Global Challenges*, 5(5):2000036.

[4] Spinoni, J., Barbosa, P., Jager, A. D., McCormick, N., Naumann, G., Vogt, J. V., Magni, D., Masante, D., Mazzeschi, M. (2019). A new global database of meteorological drought events from 1951 to 2016. *Journal of Hydrology: Regional Studies*, 22:100593.

[5] Marzi, S., Mysiak, J., Essenfelder, A. H., Pal, J. S., Vernaccini, L., Mistry, M. N., Alfieri, L., Poljansek, K., Marin-Ferrer, M., Vousdoukas, M. (2021). Assessing future vulnerability and risk of humanitarian crises using climate change and population projections within the INFORM framework. *Global Environmental Change*, 71:102393.

[6] Xiao-jun, W., Jian-yun, Z., Shahid, S., ElMahdi, A., Rui-min, H., Zhen-xin, B., Ali, M. (2012). Water resources management strategy for adaptation to droughts in China. *Mitigation and Adaptation Strategies for Global Change*, 17(8):923–937.

[7] Eckstein, G. E. (2009). Water scarcity, conflict, and security in a climate change world: challenges and opportunities for international law and policy. *Wis. Int'l LJ*, 27:409.

[8] Ndehedehe, C. E., Awange, J. L., Corner, R. J., Kuhn, M., Okwuashi, O. (2016). On the potentials of multiple climate variables in assessing the spatio-temporal characteristics of hydrological droughts over the Volta Basin. *Science of The Total Environment*, 557-558:819–837.

[9] Kazemzadeh, M., Noori, Z., Alipour, H., Jamali, S., Akbari, J., Ghorbanian, A., Duan, Z. (2022). Detecting drought events over Iran during 1983–2017 using satellite and ground-based precipitation observations. *Atmospheric Research*, 269:106052.

[10] Tadesse, T., Haile, M., Senay, G., Wardlow, B. D., Knutson, C. L. (2008). The need for integration of drought monitoring tools for proactive food security management in sub-Saharan Africa. *Natural Resources Forum*, 32(4):265–279.

[11] Senay, G. B., Velpuri, N. M., Bohms, S., Budde, M., Young, C., Rowland, J., Verdin, J. P. (2015). Drought monitoring and assessment. In *Hydro-Meteorological Hazards, Risks and Disasters*, Elsevier, 233–262.

[12] Sadeghi, M., Babaeian, E., Tuller, M., Jones, S. B. (2017). The optical trapezoid model: A novel approach to remote sensing of soil moisture applied to Sentinel-2 and Landsat-8 observations. *Remote Sensing of Environment*, 198:52–68.

[13] Qi, S., Song, B., Liu, C., Gong, P., Luo, J., Zhang, M., Xiong, T. (2022). Bamboo forest mapping in China using the dense Landsat 8 image archive and Google Earth Engine. *Remote Sensing*, 14(3):762.

[14] Ozelkan, E., Chen, G., Ustundag, B. B. (2016). Multiscale object-based drought monitoring and comparison in rainfed and irrigated agriculture from Landsat 8 OLI imagery. *International Journal of Applied Earth Observation and Geoinformation*, 44:159–170.

[15] Ali, I., Cawkwell, F., Dwyer, E., Barrett, B., Green, S. (2016). Satellite remote sensing of grasslands: from observation to management. *Journal of Plant Ecology*, 9(6):649–671.

[16] Roy, D. P., Wulder, M. A., Loveland, T. R., Woodcock, C. E., Allen, R. G., Anderson, M. C., Helder, D., Irons, J. R., Johnson, D. M., Kennedy, R., Scambos, T. A., Schaaf, C. B., Schott, J. R., Sheng, Y., Vermote, E. F., Belward, A. S., Bindschadler, R., Cohen, W. B., Gao, F., Hipple, J. D., Hostert, P., Huntington, J., Justice, C. O., Kilic, A., Kovalskyy, V., Lee, Z. P., Lymburner, L., Masek, J. G., McCorkel, J., Shuai, Y., Trezza, R., Vogelmann, J., Wynne, R. H., Zhu, Z. (2014). Landsat-8: Science and product vision for terrestrial global change research. *Remote Sensing of Environment*, 145:154–172.

[17] Bhaga, T. D., Dube, T., Shekede, M. D., Shoko, C. (2020). Impacts of climate variability and drought on surface water resources in Sub-Saharan Africa using remote sensing: a review. *Remote Sensing*, 12(24): 4184.

[18] Chinh, L. T. D., Hang, H. T. (2023). An analysis of the relative variable importance to flood fatality using a machine learning approach. *Journal of Science and Technology in Civil Engineering (STCE) - HUCE*, 17(1):125–136.

[19] Tran, H., Campbell, J., Wynne, R., Shao, Y., Phan, S. (2019). Drought and human impacts on land use and land cover change in a Vietnamese coastal area. *Remote Sensing*, 11(3):333.

[20] Trinh, L. H., Vu, D. T. (2019). Application of remote sensing technique for drought assessment based on normalized difference drought index, a case study of Bac Binh district, Binh Thuan province (Vietnam). *Russian Journal of Earth Sciences*, 19(2):1–9.

[21] Trinh, L. H., Zablotskii, V. R., Dao, K. H. (2018). A study of the long-term dynamics of soil moisture in the Bac Binh district (Binh Thuan province, Vietnam) using Landsat multispectral images. *Sovremennye problemy distantsionnogo zondirovaniya Zemli iz kosmosa*, 15(7):89–101.

[22] Das, A. C., Shahriar, S. A., Chowdhury, M. A., Hossain, M. L., Mahmud, S., Tusar, M. K., Ahmed, R., Salam, M. A. (2023). Assessment of remote sensing-based indices for drought monitoring in the northwestern region of Bangladesh. *Heliyon*, 9(2):e13016.

[23] Han, Y., Wang, Y., Zhao, Y. (2010). Estimating soil moisture conditions of the greater changbai mountains by land surface temperature and NDVI. *IEEE Transactions on Geoscience and Remote Sensing*, 48(6): 2509–2515.

[24] Du, L., Song, N., Liu, K., Hou, J., Hu, Y., Zhu, Y., Wang, X., Wang, L., Guo, Y. (2017). Comparison of two simulation methods of the temperature vegetation dryness index (TVDI) for drought monitoring in semi-arid regions of China. *Remote Sensing*, 9(2):177.

[25] Rahimzadeh-Bajgiran, P., Omasa, K., Shimizu, Y. (2012). Comparative evaluation of the Vegetation Dryness Index (VDI), the Temperature Vegetation Dryness Index (TVDI) and the improved TVDI (iTVDI) for water stress detection in semi-arid regions of Iran. *ISPRS Journal of Photogrammetry and Remote Sensing*, 68:1–12.

[26] Gao, Z., Gao, W., Chang, N.-B. (2011). Integrating temperature vegetation dryness index (TVDI) and regional water stress index (RWSI) for drought assessment with the aid of LANDSAT TM/ETM+ images. *International Journal of Applied Earth Observation and Geoinformation*, 13(3):495–503.

[27] Sarker, M., Janet, N., Mansor, S., Ahmad, B., Shahid, S., Chung, E.-S., Reid, J., Siswanto, E. (2020). An integrated method for identifying present status and risk of drought in Bangladesh. *Remote Sensing*, 12 (17):2686.

[28] Nugraha, A. S. A., Gunawan, T., Kamal, M. (2022). Modification of temperature vegetation dryness index (TVDI) method for detecting drought with multi-scale image. *IOP Conference Series: Earth and Environmental Science*, 1039(1):012048.

[29] Shashikant, V., Shariff, A. R. M., Wayayok, A., Kamal, M. R., Lee, Y. P., Takeuchi, W. (2021). Utilizing TVDI and NDWI to classify severity of agricultural drought in Chuping, Malaysia. *Agronomy*, 11(6): 1243.

[30] Deng, H., Cheng, F., Wang, J., Wang, C. (2021). Monitoring of drought in central Yunnan, China based on TVDI model. *Polish Journal of Environmental Studies*, 30(4):3511–3523.

[31] Liu, Y., Wang, S., Jiao, Z., Yang, G., Yang, Q. et al. (2018). Monitoring drought in Chaoyang County of Liaoning province using temperature vegetation drought index (TVDI). *Acta Agriculturae Zhejiangensis*, 30(1):129–136.

[32] Ngoc, H. D., Thanh, L. N. (2020). Drought risk assessment during the dry season in Tien River Estuary. *HNUE Journal of Science Natural Science*, 65(6):191–200.

[33] Mertikas, S. P., Partsinevelos, P., Mavrocordatos, C., Maximenko, N. A. (2021). Environmental applications of remote sensing. In *Pollution Assessment for Sustainable Practices in Applied Sciences and Engineering*, Elsevier, 107–163.

[34] Shamloo, N., Sattari, M. T., Apaydin, H. (2022). Agricultural drought survey using MODIS-based image indices at the regional scale: case study of the Urmia Lake Basin, Iran. *Theoretical and Applied*

Climatology, 149(1-2):39–51.

[35] Dang, T., Yue, P., Bachofer, F., Wang, M., Zhang, M. (2020). Monitoring land surface temperature change with landsat images during dry seasons in Bac Binh, Vietnam. *Remote Sensing*, 12(24):4067.

[36] Gobin, A., Hien, L. T. T., Hai, L. T., Linh, P. H., Thang, N. N., Vinh, P. Q. (2020). Adaptation to land degradation in Southeast Vietnam. *Land*, 9(9):302.

[37] Missions, L. (2016). *Using the USGS Landsat8 product*. US Department of the Interior-US Geological Survey–NASA.

[38] The USGS Earth Explorer. *Science for a changing world*. Accessed January 30, 2014; February 07, 2017; February 16, 2020.

[39] Dutta, D., Kundu, A., Patel, N. R., Saha, S. K., Siddiqui, A. R. (2015). Assessment of agricultural drought in Rajasthan (India) using remote sensing derived Vegetation Condition Index (VCI) and Standardized Precipitation Index (SPI). *The Egyptian Journal of Remote Sensing and Space Science*, 18(1):53–63.

[40] Luu, C., Bui, Q. D., Costache, R., Nguyen, L. T., Nguyen, T. T., Phong, T. V., Le, H. V., Pham, B. T. (2021). Flood-prone area mapping using machine learning techniques: a case study of Quang Binh province, Vietnam. *Natural Hazards*, 108(3):3229–3251.

[41] Ha, H., Bui, Q. D., Nguyen, H. D., Pham, B. T., Lai, T. D., Luu, C. (2022). A practical approach to flood hazard, vulnerability, and risk assessing and mapping for Quang Binh province, Vietnam. *Environment, Development and Sustainability*, 25(2):1101–1130.

[42] Kumar, B. P., Babu, K. R., Anusha, B. N., Rajasekhar, M. (2022). Geo-environmental monitoring and assessment of land degradation and desertification in the semi-arid regions using Landsat 8 OLI / TIRS, LST, and NDVI approach. *Environmental Challenges*, 8:100578.

[43] Mellon, M. (2000). High-resolution thermal inertia mapping from the mars global surveyor thermal emission spectrometer. *Icarus*, 148(2):437–455.

[44] Rongali, G., Keshari, A. K., Gosain, A. K., Khosa, R. (2018). Split-window algorithm for retrieval of land surface temperature using Landsat 8 thermal infrared data. *Journal of Geovisualization and Spatial Analysis*, 2(2).

[45] Madanian, M., Soffianian, A. R., Koupai, S. S., Pourmanafi, S., Momeni, M. (2018). The study of thermal pattern changes using Landsat-derived land surface temperature in the central part of Isfahan province. *Sustainable Cities and Society*, 39:650–661.

[46] Carlson, T. N., Ripley, D. A. (1997). On the relation between NDVI, fractional vegetation cover, and leaf area index. *Remote Sensing of Environment*, 62(3):241–252.

[47] Sandholt, I., Rasmussen, K., Andersen, J. (2002). A simple interpretation of the surface temperature/vegetation index space for assessment of surface moisture status. *Remote Sensing of Environment*, 79 (2-3):213–224.

[48] Holzman, M. E., Rivas, R., Piccolo, M. C. (2014). Estimating soil moisture and the relationship with crop yield using surface temperature and vegetation index. *International Journal of Applied Earth Observation and Geoinformation*, 28:181–192.

[49] Putri, D. N., Taqyyudin, Saraswati, R., Ash-Shidiq, I. P. (2019). Drought potential of paddy fields using temperature vegetation dryness index in kuningan regency. *E3S Web of Conferences*, 125:03009.